Available online at www.sciencedirect.com
SCIENCE DIRECT®
Journal of Mechanics and Physics of solids
53 (2005) 63–89
JOURNAL OF THE MECHANICS AND PHYSICS OF SOLIDS
www.elsevier.com/locate/jmps

Kinetic wrinkling of an elastic film on a viscoelastic substrate

R. Huang*

Research Center for Mechanics of Solids, Structures & Materials, Department of Aerospace Engineering and Engineering Mechanics, The University of Texas at Austin, Austin, TX 78712-0235, USA

Received 4 February 2004; received in revised form 17 June 2004; accepted 18 June 2004

Abstract

A compressed elastic film on a compliant substrate can form wrinkles. On an elastic substrate, equilibrium and energetics set the critical condition and select the wrinkle wavelength and amplitude. On a viscous substrate, wrinkle grows over time and the kinetics selects the fastest growing wavelength. More generally, on a viscoelastic substrate, both energetics and kinetics play important roles in determining the critical condition, the growth rate, and the wavelength. This paper studies the wrinkling process of an elastic film on a viscoelastic layer, which in turn lies on a rigid substrate. The film is elastic and modeled by the nonlinear von Karman plate theory. The substrate is linear viscoelastic with a relaxation modulus typical of a cross-linked polymer. Beyond a critical stress, the film wrinkles by the out-of-plane displacement but remains bonded to the substrate. This study considers plane strain wrinkling and neglects the in-plane displacement. A classification of the wrinkling behavior is made based on the critical conditions at the elastic limits, the glassy and rubbery states of the viscoelastic substrate. Linear perturbation analyses are conducted to reveal the kinetics of wrinkling in films subjected to intermediate and large compressive stresses. It is shown that, depending on the stress level, the growth of wrinkles at the initial stage can be exponential, accelerating, linear, or decelerating. In all cases, the wrinkle amplitude saturates at an equilibrium state after a long time. Subsequently, both amplitude and wavelength of the

*Tel: +1-512-471-7558; fax: +1-512-471-5500.
E-mail address: ruihuang@mail.utexas.edu (R. Huang).

doi:10.1016/j.jmps.2004.06.007

wrinkle evolve, but the process is kinetically constrained and slow compared to the initial growth.

Keywords: A. Buckling; B. Layered material; B. Polymeric material; B. Viscoelastic material; C. Integral transforms

1. Introduction

Recently several techniques have been developed to fabricate ordered structures at micro- and nano-scales with thin films wrinkling on compliant substrates. Bowden et al. (1998) deposited metal films on a thermally expanded polymer; upon cooling, the metal films wrinkle spontaneously. They were able to generate wrinkle patterns of complex orders over large areas by patterning polymer surfaces with bas-relief structures or by photochemically modifying planar polymer surfaces (Huck et al., 2000). Similar patterns were also generated by plasma oxidation of an elastomeric polymer, where a compressively stressed thin silicate layer forms at the surface as a result of the plasma treatment and wrinkles with wavelengths from submicrometer to micrometers (Bowden et al., 1999; Chua et al., 2000). Yoo et al. (2002) placed an elastomeric mold with periodic patterns on the surface of a metal/polymer bilayer and produced various patterns upon heating to above the glass transition temperature of the polymer, and they recently reported a spectrum of evolution of the wrinkle patterns similar to that in a spinodal system but with a longer time scale (Yoo and Lee, 2003). The capability of wrinkling has been demonstrated to be a general feature of organic–inorganic hybrid multilayer systems (Muller-Wiegand et al., 2002). Complex and ordered wrinkle patterns may offer interesting applications in fabricating micro- and nano-scale devices. On the other hand, without any control, wrinkling may be responsible for degradation of integrated devices containing organic materials (Iacopi et al., 2003). Wrinkling has also been observed in other thin film systems, such as stress relaxation of strained SiGe on a glass layer (Hobart et al., 2000; Yin et al., 2002), laser-induced surface structures of Si covered with oxides (Lu et al., 1996; Serrano and Cahill, 2002), compliant electrodes for electroactive polymer actuators (Watanabe et al., 2002), stretchable interconnects for large-area flexible electronics (Lacour et al., 2003; Jones et al., 2003), oxidation of Al-containing alloys at high temperatures (Tolpygo and Clarke, 1998), and thermal barrier coating under cyclic temperatures (Mumm et al., 2001). In nature, wrinkles develop in aging human skins as well as the skin of a shriveled apple (Cerda and Mahadevan, 2003).

The underlying mechanism of wrinkling has been generally understood as a stress-driven instability, similar to buckling of an elastic column under compression. For a solid film bonded to a substrate, however, the instability is constrained. Under compression, the film may buckle and delaminate from the substrate (Hutchinson and Suo, 1992). Alternatively, the film and the substrate stay bonded and deform concurrently to form wrinkles. This paper is concerned with the wrinkling case only.

If the substrate is elastic, there exists a critical compressive stress, beyond which the film wrinkles with a particular wavelength selected by minimizing the total elastic energy in the film and the substrate (Allen, 1969; Groenewold, 2001; Chen and Hutchinson, 2004). If the substrate is viscous, wrinkling becomes a kinetic process (Sridhar et al., 2001; Huang and Suo, 2002a). In this case, since the viscous substrate does not store elastic energy, a compressed blanket film is always unstable energetically. The viscous flow in the substrate controls the kinetics, selecting a fastest growing wavelength. Other kinetic processes associated with wrinkling include interfacial diffusion (Suo, 1995), nonlinear creep of substrate (Balint and Hutchinson, 2003), and plastic ratcheting under cyclic temperatures (He et al., 2000; Karlsson and Evans, 2001; Im and Huang, 2004).

This paper studies wrinkling of an elastic film on a viscoelastic substrate with a relaxation modulus typical of a cross-linked polymer. As opposed to elastic and viscous substrates in previous studies, the viscoelastic substrate has a profound effect on both energetics and kinetics of wrinkling. The paper is organized as follows. Section 2 outlines the model with elastic deformation of the film, viscoelastic deformation of the substrate, and coupling between them. Section 3 presents the equilibrium and energetics for wrinkling of an elastic film on an elastic substrate. In Section 4, a classification of the wrinkling behavior on viscoelastic substrates is made based on the energetics at the elastic limits, the glassy and rubbery states of the viscoelastic substrates; the kinetics of wrinkling is then studied by linear perturbation analyses, starting from a flat film and a wrinkled film, respectively, subjected to intermediate and large compressive stresses. The study develops a unifying map for wrinkling behavior of compressed elastic films on viscoelastic substrates, with elastic and viscous substrates as two limiting cases. The results may be used to characterize the viscoelastic properties of thin polymer films or to devise new techniques for fabricating ordered structures at micro- and nano-scales.

2. The model

Fig. 1 schematically illustrates the structure under consideration: an elastic film of thickness h_f bonded to a viscoelastic layer of thickness H, which in turn lies on a rigid substrate. At the reference state (Fig. 1a), the film is flat and subjected to a biaxial compressive residual stress (i.e., $\sigma_0 < 0$). Upon wrinkling (Fig. 1b), the film deforms elastically to relax the compressive stress, and the viscoelastic layer deforms concurrently to maintain perfect bonding at the interface. We consider plane-strain deformation only.

2.1. Elastic deformation of the film

We employ the nonlinear von Karman plate theory (Timoshenko and Woinowsky-Krieger, 1987; Landau and Lifshitz, 1959) to model the elastic film. The plane-strain elastic deformation of the film is described by a deflection w and an in-plane displacement u. The top surface of the film is traction free, and the bottom

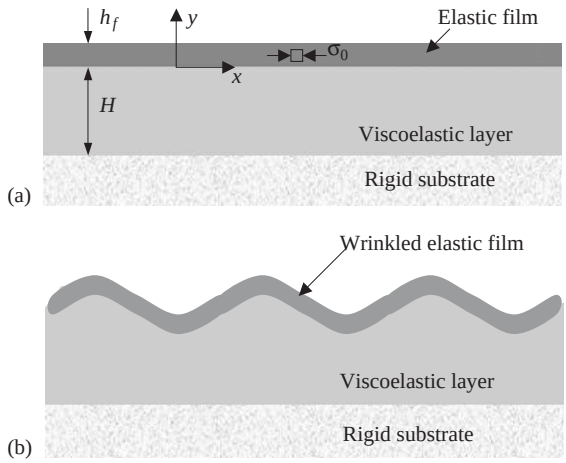

Fig. 1. A schematic of the model structure: (a) reference state; (b) wrinkled state.

surface, bonded to the substrate, is subjected to both normal and shear tractions. At equilibrium, the pressure p (negative normal traction) and the shear traction T are, respectively

$$p = \frac{E_f h_f^3}{12(1-\nu_f^2)}\frac{\partial^4 w}{\partial x^4} - N\frac{\partial^2 w}{\partial x^2} - T\frac{\partial w}{\partial x}, \tag{2.1}$$

$$T = \frac{\partial N}{\partial x}, \tag{2.2}$$

where E_f is the Young's modulus of the film, ν_f is the Poisson's ratio, and N is the in-plane membrane force given by

$$N = \sigma_0 h_f + \frac{E_f h_f}{1-\nu_f^2}\left[\frac{\partial u}{\partial x} + \frac{1}{2}\left(\frac{\partial w}{\partial x}\right)^2\right]. \tag{2.3}$$

Note that, both the in-plane displacement and the deflection contribute to the in-plane membrane force and thus the relaxation of the initial compressive stress. In particular, the nonlinear term in (2.3) accounts for the length change of the film due to the large deflection of the film compared to its thickness.

Previous studies (Huang and Suo, 2002a, b) have shown that, while in-plane displacement and the shear traction have some effects on wrinkling behavior, up to a factor of 4 in some cases, including them in the analysis is tedious and often leads to lengthy solutions not convenient for practical use. On the other hand, a common approximation is to ignore the in-plane displacement and the shear traction (Ortiz and Gioia, 1994; Gioia et al., 2002; Sridhar et al., 2002; Balint and Hutchinson, 2003). The nonlinearity is retained to the leading order by considering the average length change of the film due to large deflection. Consider a sinusoidal wrinkle with

amplitude A and wavelength $L = 2\pi/k$, namely

$$w = A \cos kx. \tag{2.4}$$

The average membrane force is given by

$$N_a = \sigma_0 h_f + \frac{E_f h_f}{1 - \nu_f^2} \frac{1}{L} \int_0^L \frac{1}{2} \left(\frac{\partial w}{\partial x} \right)^2 dx. \tag{2.5}$$

Inserting (2.4) into (2.5) and then into (2.1), we obtain that

$$p = \frac{E_f A}{12(1 - \nu_f^2) h_f} \left[\frac{12(1 - \nu_f^2)\sigma_0}{E_f} k^2 h_f^2 + k^4 h_f^4 \left(1 + 3 \frac{A^2}{h_f^2} \right) \right] \cos kx. \tag{2.6}$$

It will be noted that this approximation leads to a slightly different equilibrium wrinkle amplitude for an elastic substrate but identical amplitude for a viscous substrate compared to previous studies. We caution that a more rigorous analysis should include the effects of the in-plane displacement and the shear traction for both linear and nonlinear analysis.

2.2. Viscoelastic deformation of the substrate

The substrate is assumed to be isotropic, linear viscoelastic. The stress–strain relation takes an integral form (Christensen, 1982):

$$\sigma_{ij}(t) = 2 \int_{-\infty}^{t} \mu(t - \tau) \frac{\partial \varepsilon_{ij}(\tau)}{\partial \tau} d\tau + \delta_{ij} \int_{-\infty}^{t} \lambda(t - \tau) \frac{\partial \varepsilon_{kk}(\tau)}{\partial \tau} d\tau, \tag{2.7}$$

where $\mu(t)$ and $\lambda(t)$ are the viscoelastic relaxation moduli. For an elastic substrate, Eq. (2.7) reduces to Hooke's law as the relaxation moduli are independent of time. The Latin indices take values 1, 2, and 3, and a repeated index implies summation over 1, 2, and 3. Assuming no body force and neglecting inertia for quasi-static deformation, equilibrium requires that

$$\frac{\partial \sigma_{ij}}{\partial x_j} = 0. \tag{2.8}$$

Assuming small deformation, the strain-displacement relation is

$$\varepsilon_{ij} = \frac{1}{2} \left(\frac{\partial u_i}{\partial x_j} + \frac{\partial u_j}{\partial x_i} \right). \tag{2.9}$$

Eqs. (2.7)–(2.9) form a complete set of governing equations for linear viscoelasticity.

Consider plane-strain deformation of the substrate. The initial condition is taken to be stress free. The boundary conditions are

$$\sigma_{21} = S_1(x, t), \quad \sigma_{22} = S_2(x, t) \text{ at } y = 0; \tag{2.10}$$

$$u_2 = u_1 = 0 \quad \text{at } y = -H. \tag{2.11}$$

Condition (2.11) assumes fixed boundary at the bottom, and (2.10) assumes a normal and a shear tractions at the top surface. To specialize, we consider the following

tractions:

$$S_1(x,t) = A_1(t)\sin kx, \tag{2.12}$$

$$S_2(x,t) = A_2(t)\cos kx, \tag{2.13}$$

where k is the wave number of the periodic traction, and A_1 and A_2 are the time-dependent amplitudes.

We solve the above viscoelastic boundary value problem by the integral transform method (Christensen, 1982). The Laplace transform of (2.7) is

$$\bar{\sigma}_{ij}(s) = 2s\bar{\mu}(s)\bar{\varepsilon}_{ij}(s) + s\bar{\lambda}_{ij}(s)\bar{\varepsilon}_{kk}(s)\delta_{ij}, \tag{2.14}$$

where a bar over a variable designates its Laplace transform, and s is the transform variable. The Laplace transforms of Eqs. (2.8) and (2.9) have the same form as their originals and are not repeated. The Laplace transform of the boundary conditions are

$$\bar{\sigma}_{21} = \bar{A}_1(s)\sin kx, \quad \bar{\sigma}_{22} = \bar{A}_2(s)\cos kx \text{ at } y = 0; \tag{2.15}$$

$$\bar{u}_2 = \bar{u}_1 = 0 \text{ at } y = -H. \tag{2.16}$$

The solution to the Laplace transformed viscoelastic problem can be obtained directly from the solution to the corresponding elastic problem by replacing the elastic moduli μ and λ with $s\bar{\mu}$ and $s\bar{\lambda}$, respectively, the so-called elastic–viscoelastic correspondence principle. The final solution will be realized upon inverting the transformed solution. For the present problem, the corresponding elastic solution is presented in Appendix A, from which we obtain the Laplace transformed displacements at the surface of the substrate (i.e., $y = 0$)

$$\bar{u}_1(x,0,s) = \frac{1}{2ks\bar{\mu}(s)}\left[\gamma_{11}(s\bar{\nu},kH)\bar{A}_1(s) + \gamma_{12}(s\bar{\nu},kH)\bar{A}_2(s)\right]\sin(kx), \tag{2.17}$$

$$\bar{u}_2(x,0,s) = \frac{1}{2ks\bar{\mu}(s)}\left[\gamma_{21}(s\bar{\nu},kH)\bar{A}_1(s) + \gamma_{22}(s\bar{\nu},kH)\bar{A}_2(s)\right]\cos(kx), \tag{2.18}$$

where the dimensionless coefficients γ_{ij} are given by (A.13)–(A.15) with $\kappa = 3 - 4s\bar{\nu}(s)$ and $\bar{\nu}(s)$ is the Laplace transform of the Poisson's ratio of the substrate.

The coupling between (2.17) and (2.18) indicates that, in general, the surface of the substrate undergoes both out-of-plane and in-plane displacements, even in the cases with no shear tractions at the surface. Only in one special case, when the substrate is infinitely thick ($kH \to \infty$) and incompressible ($\nu = 0.5$), $\gamma_{12} = \gamma_{21} = 0$, are the two equations decoupled. Nevertheless, in the same spirit of approximation taken for the elastic deformation of the film, we neglect the in-plane displacement at the surface of the substrate. Thus, (2.18) becomes

$$\bar{u}_2(x,0,s) = \frac{\gamma_{22}(s\bar{\nu},kH)}{2ks\bar{\mu}(s)}\bar{S}_2(x,s). \tag{2.19}$$

The inverse Laplace transform of (2.19) leads to a relation between the normal traction at the surface and the out-of-plane surface displacement, which will be coupled with the elastic deformation of the film as below.

2.3. Coupling between the film and the substrate

Assuming that the film and the substrate are perfectly bonded at the interface, the displacements and the tractions are continuous across the interface, namely

$$u_2(x,0,t) = w(x,t), \tag{2.20}$$

$$S_2(x,t) = -p(x,t). \tag{2.21}$$

The above conditions, together with (2.6) and (2.19), form a coupled problem that is nonlinear and time-dependent.

3. Elastic substrates: equilibrium and energetics

Wrinkling of an elastic film on an elastic substrate has been studied previously (e.g., Allen, 1969; Groenewold, 2001; Chen and Hutchinson, 2004). Here we rederive the essential results, which play several roles in the present study. For an elastic substrate, as a special case, the inverse transform of (2.19) gives

$$u_2(x,0) = \frac{\gamma_{22}(v,kH)}{2k\mu} S_2(x), \tag{3.1}$$

which is the equilibrium condition of the substrate. Applying the continuity conditions (2.20) and (2.21) and the equilibrium condition of the film (2.6), we obtain

$$A_e = \frac{2\sqrt{1-v_f^2}}{k}\left[-\frac{\sigma_0}{E_f} - \frac{(kh_f)^2}{12(1-v_f^2)} - \frac{2}{\gamma_{22}}\frac{\mu}{E_f}\frac{1}{kh_f}\right]^{1/2}, \tag{3.2}$$

where A_e designates the equilibrium amplitude of the wrinkle. Note that the equilibrium amplitude (3.2) is slightly larger than that obtained from energy minimization (e.g., Eq. (B.8) in Appendix B). The difference is due to the approximation made in the equilibrium analysis, where the average membrane force (2.5) is used. A more rigorous analysis would require a non-sinusoidal wrinkle at equilibrium, which will not be pursued here. Interestingly, the equilibrium amplitude reduces to that for a pure viscous substrate by setting $\mu = 0$ (Huang and Suo, 2002a, b). Also note that (3.2) includes the effect of substrate thickness through the coefficient γ_{22}, given by (A.14) in Appendix A. Fig. 2 plots the coefficient as a function of H/L, the ratio between the substrate thickness and the wrinkle wavelength ($L = 2\pi/k$), for various Poisson's ratios of the substrate. Evidently, the effect of substrate thickness diminishes if $H/L > 1$. At the limit of a thick substrate, the coefficient depends on the Poisson's ratio of the substrate as $\gamma_{22} = 2(1-v)$.

The three terms in the bracket of (3.2) compete to determine the stability of the film. The first term, positive for a compressed film ($\sigma_0 < 0$), promote wrinkling to relax the in-plane compression. The second term, always negative, disfavors small wavelength wrinkles due to the flexural rigidity of the film. The third term, also negative, disfavors long wavelength wrinkles due to the elastic constraint of the

substrate. The film is flat and stable if the last two terms win the competition over the first term for all wavelengths. Otherwise, the film forms wrinkle at an intermediate wavelength. Fig. 3 plots the equilibrium wrinkle amplitude as a function of wavelength for three different combinations of film stress and substrate stiffness. For each combination, there exists a wavelength window, within which a non-zero equilibrium amplitude exists. Outside the window, the equilibrium amplitude is zero. The window shrinks as the substrate modulus increases and/or the compressive film stress decreases. A critical condition exists, under which the equilibrium amplitude is

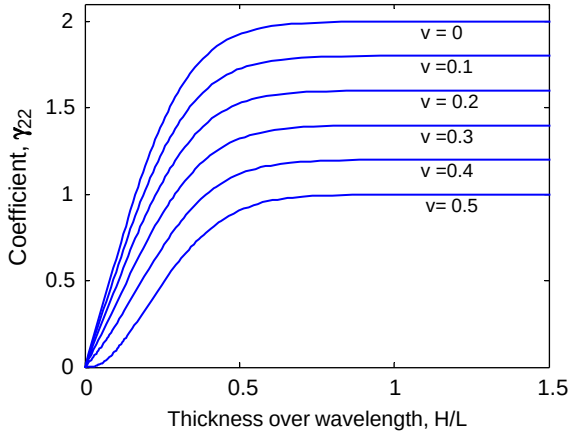

Fig. 2. Effect of substrate thickness (H) and Poisson's ratio (ν).

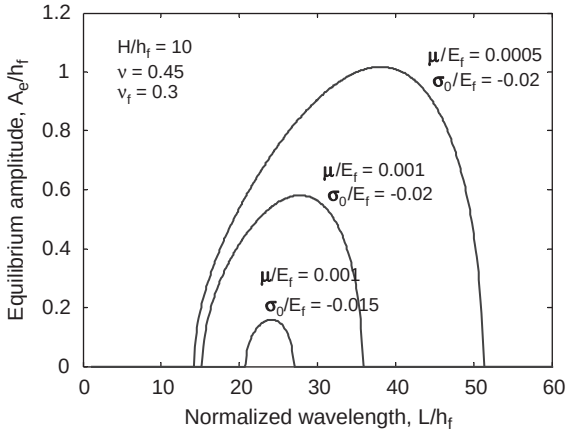

Fig. 3. Equilibrium wrinkle amplitude as a function of wavelength for elastic films ($\nu_f = 0.3$) on elastic substrates ($\nu = 0.45$) with various combinations of film stress and stiffness ratios and a thickness ratio $H/h_f = 10$.

zero for all wavelengths and a flat film is stable. The stability condition can be obtained by setting the maximum amplitude of (3.2) to zero, which in general takes the form

$$f\left(\frac{\sigma_0}{E_f}, \frac{\mu}{E_f}, \frac{H}{h_f}, \nu, \nu_f\right) = 0. \tag{3.3}$$

For the limiting case of a thick substrate ($H \to \infty$), the critical condition reduces to

$$\left(\frac{\sigma_0}{E_f}\right)^3 + \frac{9}{16(1-\nu_f^2)(1-\nu)^2}\left(\frac{\mu}{E_f}\right)^2 = 0. \tag{3.4}$$

For the other limiting case of a thin substrate ($H \to 0$), the critical condition reduces to

$$\left(\frac{\sigma_0}{E_f}\right)^2 - \frac{2(1-\nu)}{3(1-\nu_f^2)(1-2\nu)}\frac{\mu}{E_f}\frac{h_f}{H} = 0. \tag{3.5}$$

Fig. 4 plots the critical condition in the plane of the normalized film stress, σ_0/E_f, versus the stiffness ratio, μ/E_f, for various thickness ratios between the substrate and the film. Each line divides the plane into two regions: below the line, the flat film is stable; above the line, the film wrinkles. For given film and substrate materials, the critical condition predicts the minimum compressive stress for the film to wrinkle. For a given compressive stress in the film, the critical condition predicts the maximum substrate stiffness for the film to wrinkle. The close form solutions for the limiting cases are plotted in Fig. 4: Eq. (3.4) as dashed lines and Eq. (3.5) as dotted lines for $H/h_f = 0.1$. We observe that, for the thickness ratio bigger than 10, the substrate thickness has little effect on the critical condition, and (3.4) can be used. On

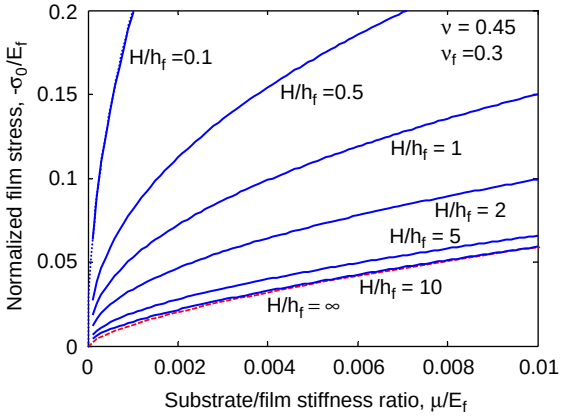

Fig. 4. Critical condition of wrinkling for elastic films ($\nu_f = 0.3$) on elastic substrates ($\nu = 0.45$) with various thickness ratios. The dashed line is for the limiting case of thick substrates (Eq. 3.4), and the dotted line is for the limiting case of thin substrate (Eq. 3.5) with the thickness ratio $H/h_f = 0.1$.

the other hand, because a fixed boundary condition has been assumed at the bottom of the substrate, a thinner substrate provides more constraints for wrinkling, and thus larger critical stress. Alternatively, if the bottom of the substrate were free of tractions, the effect of substrate thickness would be the opposite.

The above solution is obtained from equilibrium consideration, which predicts the stability condition and the equilibrium wrinkle amplitude. For a blanket film, there exist infinitely many equilibrium states, with intermediate wavelengths bounded by two limits as shown in Fig. 3. Equilibrium does not select a particular wavelength. As in the case of a solid bar under compression, the buckling wavelength depends on the boundary condition and minimizes the strain energy. For a blanket film without any in-plane boundary condition, an energetic consideration selects the wavelength that minimizes the total free energy. Appendix B presents an energetic analysis, which selects a wavelength, $L_m = 2\pi/k_m$, with k_m in the form of Eq. (B.9). The wavelength is a function of the moduli, Poisson's ratios, and thicknesses of both the substrate and the film, but independent of the compressive stress. Fig. 5 plots the selected wavelength as a function of the stiffness ratio, μ/E_f, for various thickness ratios. The corresponding equilibrium amplitude increases as the compressive stress in the film increases, as shown in Fig. 6. The amplitude is zero below a critical stress and increases monotonically as the substrate stiffness decreases. The critical stress can be obtained from the critical condition, Eq. (3.4) for a thick substrate.

The equilibrium and energetics analyses above predict the stability condition, selected wrinkle wavelength and amplitude for elastic films on elastic substrates, which agrees with previous studies for the limiting case of thick substrates (e.g., Allen, 1969; Groenewold, 2001) and, in addition, includes the effect of substrate thickness and Poisson's ratio.

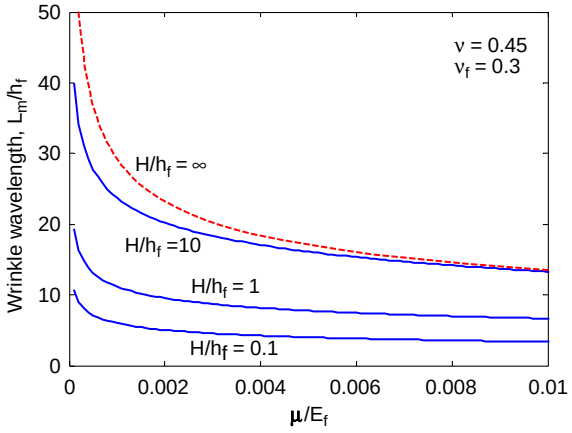

Fig. 5. Selected wrinkle wavelength for elastic films ($\nu_f = 0.3$) on elastic substrates ($\nu = 0.45$) with various thickness ratios. The dashed line is for the limiting case of thick substrates, where the wave number is given by Eq. (B.10).

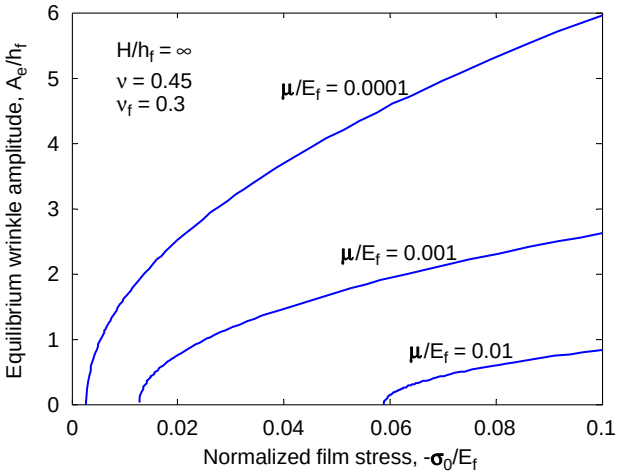

Fig. 6. Equilibrium wrinkle amplitude of the selected wavelength for elastic films ($\nu_f = 0.3$) on thick elastic substrates ($H/h_f \to \infty$, $\nu = 0.45$) with various stiffness ratios.

4. Viscoelastic substrates: classification and kinetics

For a viscoelastic substrate, the relaxation modulus, $\mu(t)$, is a function of time (Fig. 7), with the glassy modulus $\mu(0) = \mu_0$ and the rubbery modulus $\mu(\infty) = \mu_\infty$. For a typical cross-linked polymer, the modulus varies by four orders of magnitude: $\mu_0 \sim 10^9$ Pa and $\mu_\infty \sim 10^5$ Pa. In general, the Poisson's ratio is also a function of time, but the time dependence is much weaker. Here we assume that the Poisson's ratio is a constant, independent of time. Wrinkling of an elastic film on such a viscoelastic substrate becomes a kinetic process. Nevertheless, a classification of the wrinkling behavior can be made based on the solution for elastic substrates.

At the initial stage ($t = 0^+$), the glassy state prevails; the critical condition (3.3) predicts a critical film stress. For a thick substrate, from Eq. (3.4), the critical stress is

$$\sigma_{c0} = -E_f \left(\frac{9}{16(1-\nu_f^2)(1-\nu)^2} \right)^{1/3} \left(\frac{\mu_0}{E_f} \right)^{2/3}. \tag{4.1}$$

At time $t = \infty$, the rubbery state prevails, and the critical stress is

$$\sigma_{c\infty} = -E_f \left(\frac{9}{16(1-\nu_f^2)(1-\nu)^2} \right)^{1/3} \left(\frac{\mu_\infty}{E_f} \right)^{2/3}. \tag{4.2}$$

For a typical cross-linked polymer, the two critical stresses differ by two orders of magnitude.

We now classify the wrinkling behavior of elastic films on viscoelastic substrates. If the compressive stress in the film is small ($|\sigma_0| < |\sigma_{c\infty}|$), the flat film is stable at both

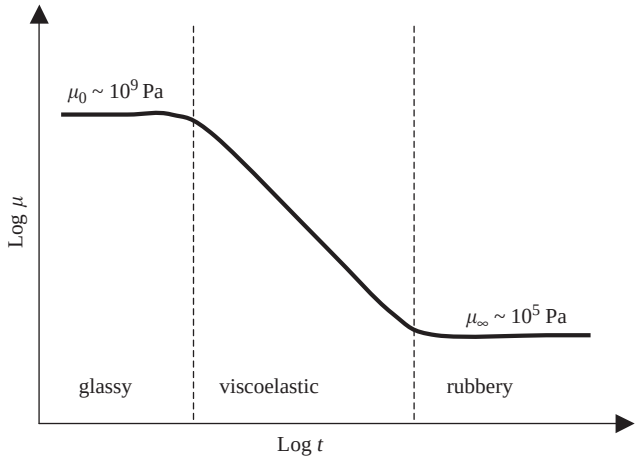

Fig. 7. A schematic of the relaxation modulus as a function of time for a viscoelastic material.

glassy and rubbery states. Consequently, the film does not wrinkle at all. On the other hand, if the film stress is large ($|\sigma_0| > |\sigma_{c0}|$), the film wrinkles immediately at the glassy state. As time goes on, the wrinkle amplitude grows as the substrate softens. Meanwhile, the wavelength of the wrinkle evolves, from the selected wavelength at the glassy state to that at the rubbery state. Consider thick substrates only. From Eq. (B.10), the selected wavelength is

$$L_0 = 2\pi h_f \left[\frac{1-\nu}{6(1-\nu_f^2)}\frac{E_f}{\mu_0}\right]^{1/3} \tag{4.3}$$

at the glassy state, and is

$$L_\infty = 2\pi h_f \left[\frac{1-\nu}{6(1-\nu_f^2)}\frac{E_f}{\mu_\infty}\right]^{1/3} \tag{4.4}$$

at the rubbery state. For a typical cross-linked polymer, the wavelength increases by more than an order of magnitude ($L_\infty/L_0 \sim 20$). For the third case, if the film stress is intermediate ($|\sigma_{c\infty}| < |\sigma_0| < |\sigma_{c0}|$), the flat film is energetically stable at the glassy state but unstable at the rubbery state. As will be shown by a kinetic analysis later, the film starts to grow wrinkle even at the glassy state and the growth rate depends on the viscoelastic behavior of the substrate. A viscous substrate is a limiting case, where $\mu_0 = \infty$ and $\mu_\infty = 0$. Previous studies (Sridhar et al., 2001; Huang and Suo, 2002a) have shown that a compressed elastic film wrinkles kinetically on a viscous substrate.

Fig. 8 depicts a map of the wrinkling behavior on the plane spanned by the compressive stress in the film and the wrinkle amplitude. The two equilibrium amplitudes at the elastic limits for the glassy and rubbery states divide the plane into three regions. In region I, the film wrinkles instantaneously at the glassy state, a

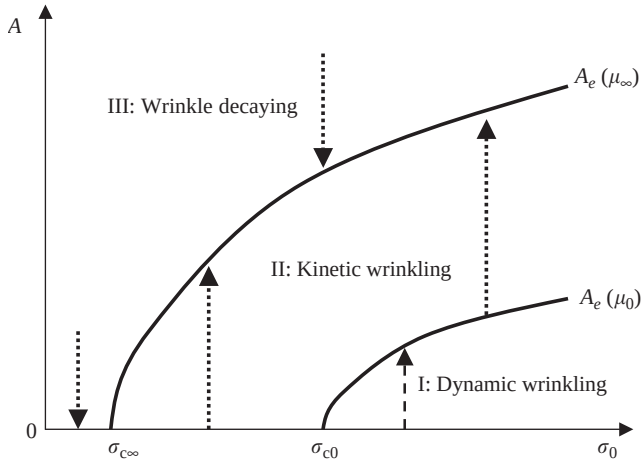

Fig. 8. A schematic map of the wrinkling behavior of elastic films on viscoelastic substrates. The two solid lines correspond to the equilibrium amplitudes at the glassy and rubbery states, respectively.

dynamic process. In region II, wrinkle grows gradually, a kinetic process. In region III, wrinkles (if any) decay. In the following we focus on the kinetics of wrinkling in region II, which is directly related to the viscoelastic behavior of the substrate. Depending on the compressive stress in the film, the kinetic wrinkling can either start from a flat film or start from a wrinkled film following the instantaneous wrinkling at the glassy state. The two cases have different kinetics and will be studied separately.

4.1. Kinetics of wrinkling I: intermediate stress

Consider an elastic film subjected to an intermediate compressive stress ($|\sigma_{c\infty}|<|\sigma_0|<|\sigma_{c0}|$). Start from the reference state with a flat film (Fig. 1a). Assume a sinusoidal perturbation in the form of Eq. (2.4), now with a time-dependent amplitude, $A(t)$. The pressure at the film/substrate interface is given by Eq. (2.6). For linear perturbation analysis, neglecting the higher order terms of A, we obtain

$$p(x,t)=\frac{E_f}{12(1-\nu_f^2)}\left[\frac{12(1-\nu_f^2)\sigma_0}{E_f}k^2h_f^2+k^4h_f^4\right]\frac{A(t)}{h_f}\cos kx. \tag{4.5}$$

Let $B(t)=\mathrm{d}A/\mathrm{d}t$ and the corresponding Laplace transform $\bar{B}(s)=s\bar{A}(s)-A_0$, where A_0 is the initial amplitude. Applying the continuity conditions (2.20) and (2.21) and inserting into Eq. (2.19), we obtain

$$\bar{B}(s)=\frac{\alpha E_f}{\bar{\mu}(s)}\bar{A}(s)-A_0, \tag{4.6}$$

where

$$\alpha = \frac{\gamma_{22}(v, kH)}{24(1-v_f^2)kh_f}\left[-k^4h_f^4 - \frac{12(1-v_f^2)\sigma_0}{E_f}k^2h_f^2\right]. \tag{4.7}$$

We have assumed that Poisson's ratio of the substrate (v) is independent of time. The inverse Laplace transform of Eq. (4.6) leads to an integro-differential equation governing the growth of the perturbation. In general, numerical methods must be used to solve the integro-differential equation. In the following, we obtain analytical solutions for a specific viscoelastic behavior of the substrate.

Experimentally measured viscoelastic relaxation modulus $\mu(t)$ can be interpreted in terms of a mechanical model consisting of an array of spring-dashpot analogs in parallel (Fig. 9). To ensure a rubbery elastic limit, one of the parallel branches must be a spring of modulus μ_∞, with no dashpot. Each of the other parallel branches comprises a spring of modulus μ_i and a dashpot of viscosity η_i. The model leads to the relaxation modulus

$$\mu(t) = \mu_\infty + \sum_i \mu_i \exp(-p_i t), \tag{4.8}$$

where $p_i = \mu_i/\eta_i$ is the relaxation parameter of one branch. The Laplace transform of the relaxation modulus is

$$\bar{\mu}(s) = \frac{\mu_\infty}{s} + \sum_i \frac{\mu_i}{s+p_i}. \tag{4.9}$$

In the following, we use only the first two terms of Eq. (4.8) for the relaxation modulus. Substituting the first two terms of Eq. (4.9) into Eq. (4.6) and rearranging with the relation $\bar{B}(s) = s\bar{A}(s) - A_0$, we obtain

$$\bar{B}(s) = \frac{\alpha E_f - \mu_\infty}{\mu_0 - \alpha E_f} p_1 \bar{A}(s) - A_0, \tag{4.10}$$

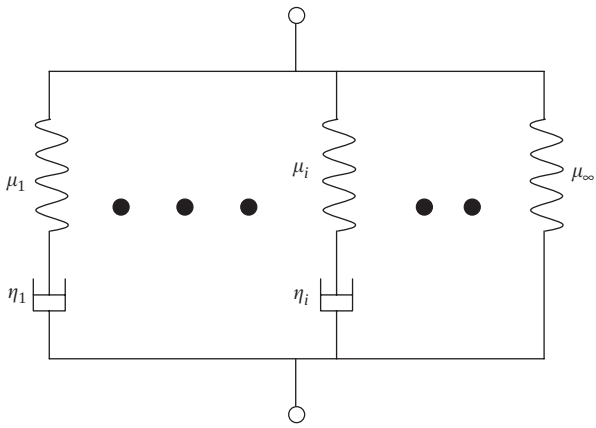

Fig. 9. A mechanical model of viscoelastic substrates.

where $\mu_0 = \mu_\infty + \mu_1$ is the glassy modulus. The inverse Laplace transform of Eq. (4.10) is

$$\frac{dA}{dt} = \frac{\alpha E_f - \mu_\infty}{\mu_0 - \alpha E_f} p_1 A(t), \tag{4.11}$$

which is an ordinary differential equation that has a solution in the form of an exponential function, namely

$$A(t) = A_0 \exp\left[\frac{\alpha E_f - \mu_\infty}{\mu_0 - \alpha E_f} p_1 t\right]. \tag{4.12}$$

Equation (4.12) indicates that, at the initial stage, the wrinkle either grows or decays exponentially, depending on the sign of the coefficient, $\beta = (\alpha E_f - \mu_\infty)/(\mu_0 - \alpha E_f)$, which in turn depends on the compressive stress in the film and the wrinkle wavelength. When the film stress is small ($|\sigma_0| < |\sigma_{c\infty}|$), the coefficient is negative for all wavelengths; a flat film is stable. For an intermediate film stress ($|\sigma_{c\infty}| < |\sigma_0| < |\sigma_{c0}|$), the coefficient is positive within a window bounded by two critical wavelengths (Fig. 10). A fastest growing mode exists within the window, which dominates the initial growth. The above linear perturbation analysis does not apply for the case with a large film stress ($|\sigma_0| > |\sigma_{c0}|$) because the film wrinkles instantaneously at the glassy state, which will be considered in the next section.

As a limiting case, if the substrate is viscous with a constant viscosity η, the relaxation modulus is a delta function, $\mu(t) = \eta\delta(t)$, and Eq. (4.12) reduces to (with $\mu_\infty = 0$, $\mu_0 = \infty$, and $\mu_0/p_1 = \eta$)

$$A(t) = A_0 \exp\left[\frac{\alpha E_f}{\eta} t\right], \tag{4.13}$$

which is identical to the solution in Sridhar et al. (2001). Similarly, Eq. (4.12) can be reduced for simpler viscoelastic models, such as Maxwell model ($\mu_\infty = 0$) and Kelvin model ($\mu_0 = \infty$).

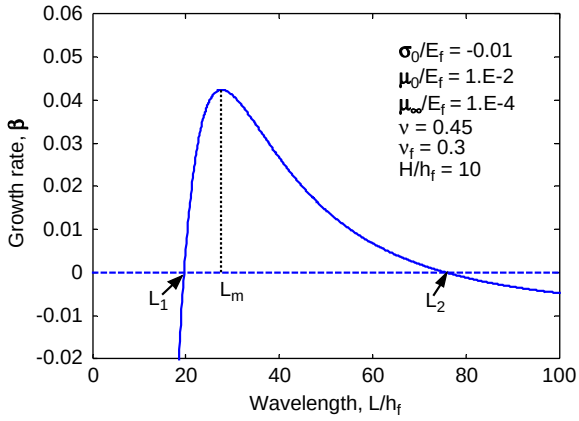

Fig. 10. Normalized growth rate, $\beta = (\alpha E_f - \mu_\infty)/(\mu_0 - \alpha E_f)$, as a function of the wrinkle wavelength for an elastic film, subjected to an intermediate compressive stress, on a viscoelastic substrate.

While energetics selects the wrinkle wavelength on an elastic substrate, kinetics selects the fastest growing mode on a viscoelastic substrate. The wavelength of the fastest growing mode can be obtained by setting $\partial\beta/\partial k = 0$, or equivalently, $\partial\alpha/\partial k = 0$. For a thick substrate, we obtain

$$L_{\mathrm{m}} = \pi h_{\mathrm{f}} \sqrt{-\frac{E_{\mathrm{f}}}{(1-\nu_{\mathrm{f}}^2)\sigma_0}}. \tag{4.14}$$

Note that the wavelength of the fastest growing mode is independent of the substrate. Namely, the kinetics selects the same wavelength whether the substrate is viscous or viscoelastic. Differing from an elastic substrate, the kinetically selected

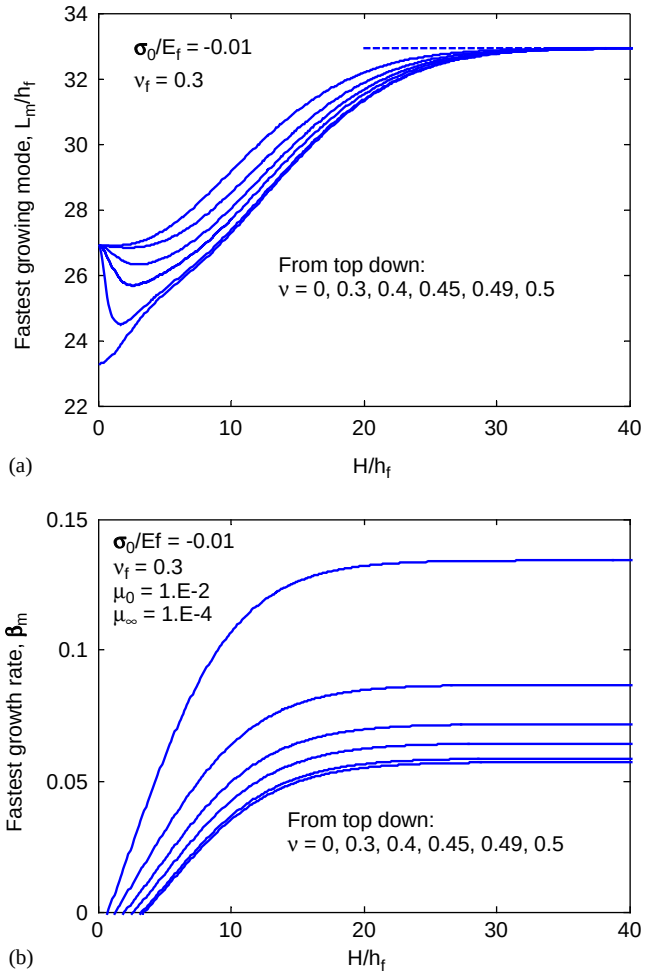

Fig. 11. (a) The wavelength and (b) the growth rate of the fastest growing wrinkle of an elastic film on a viscoelastic substrate.

wavelength depends on the compressive stress in the film. For a thin viscoelastic substrate, the selected wavelength weakly depends on the substrate thickness and Poisson's ratio, as shown in Fig. 11a. Fig. 11b plots the corresponding growth rate. A critical thickness exists, below which the growth rate is negative and a flat film is stable. While the relaxation modulus does not play a role in selecting the fastest growing mode, it is important in determining the corresponding growth rate. The growth rate scales with the relaxation parameter p_1 and depends on the glassy and rubbery moduli. As shown in Fig. 12 for a thick substrate ($H/h_f = 40$), the fastest growth rate approaches infinity as the glassy modulus decreases, entering the regime of dynamic wrinkling as the critical stress σ_{c0} drops below the compressive stress in the film σ_0 (Region I of Fig. 8). At the other end, the growth rate approaches zero as the rubbery modulus increases and become negative as the critical stress $\sigma_{c\infty}$ rises beyond σ_0, entering the regime of no wrinkling (Region III of Fig. 8). The growth rate increases as the ratio between the rubbery modulus and the glassy modulus decreases, but the effect diminishes as the ratio drops below 0.001.

The linear perturbation analysis above is only valid at the initial stage of wrinkling. Nonlinear analysis is necessary for long time evolution. Nevertheless, the evolution process can be understood as follows. At the beginning, the wrinkle grows exponentially and the fastest growing mode (L_m) dominates. The growth slows down as the amplitude becomes large compared to the film thickness, and eventually saturates at an equilibrium amplitude corresponding to that for an elastic substrate with the rubbery modulus. Fig. 13 schematically illustrates the evolution of wrinkle amplitude as a function of time. A similar behavior was shown by a nonlinear analysis for an elastic film on a viscous substrate (Huang and Suo, 2002a), and was experimentally observed (Yin et al., 2002). Subsequently, the wrinkle evolves toward the energetically selected mode at the rubbery state with the wavelength L_∞ and the

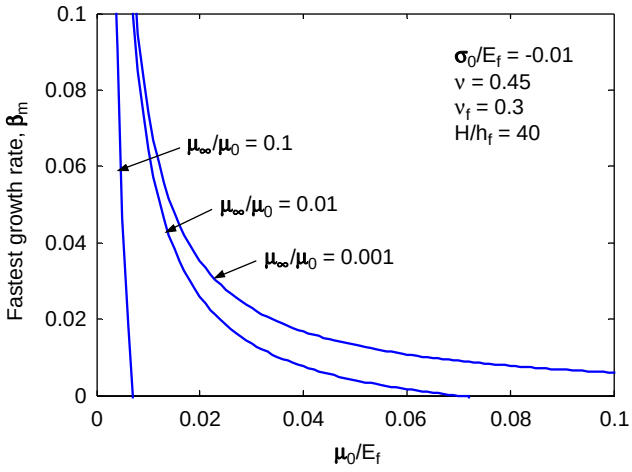

Fig. 12. The normalized growth rate of the fastest growing wrinkle of an elastic film on a thick viscoelastic substrate with varying glassy and rubbery moduli.

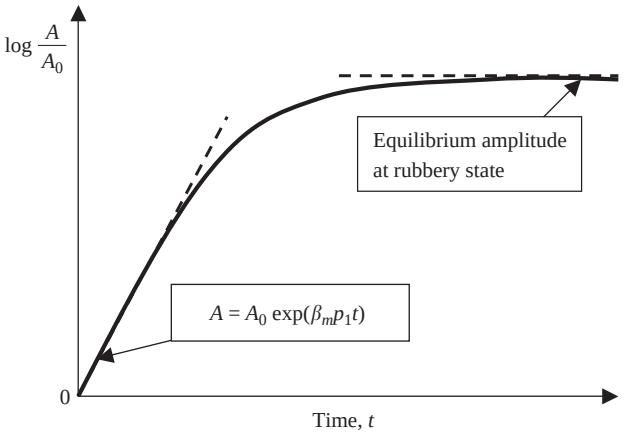

Fig. 13. A schematic of the growth of wrinkle amplitude.

corresponding equilibrium amplitude. The transition of the wrinkling wavelength from L_m to L_∞ is slow due to the kinetic constraint of the substrate. A similar transition has been observed in experiments (Muller-Wiegand et al., 2002; Yoo and Lee, 2003).

4.2. Kinetics of wrinkling II: large stress

For a film subjected to a large compressive stress (i.e., $|\sigma_0| > |\sigma_{c0}|$), the film wrinkles instantaneously to an equilibrium state at the glassy state. For a thick substrate ($H/h_f \to \infty$), the wavelength L_0 is given by (4.3), and the corresponding equilibrium amplitude A_0 is, from (3.2),

$$A_0 = h_f \sqrt{\frac{\sigma_0}{\sigma_{c0}} - 1}, \tag{4.15}$$

where σ_{c0} is given by Eq. (4.1). The wrinkle grows as the viscoelastic substrate softens over time. Assume a small perturbation, namely

$$w(x,t) = [A_0 + \delta(t)] \cos\left(\frac{2\pi x}{L_0}\right), \tag{4.16}$$

where $\delta(t) \ll A_0$. Substituting Eq. (4.16) into Eq. (2.6) and keeping the leading terms of $\delta(t)$ only, we obtain that

$$p(x,t) = p_0 \cos k_0 x + \frac{E_f}{12(1-\nu_f^2)} \left[\frac{12(1-\nu_f^2)\sigma_0}{E_f} k_0^2 h_f^2 + k_0^4 h_f^4 \left(1 + 9\frac{A_0^2}{h_f^2}\right) \right] \times \frac{\delta(t)}{h_f} \cos k_0 x, \tag{4.17}$$

where $k_0 = 2\pi/L_0$, and p_0 is the pressure when $\delta = 0$. For a thick substrate, using Eqs. (4.3) and (4.15), we obtain that

$$p_0 = -\frac{\mu_0}{1-\nu} k_0 A_0. \tag{4.18}$$

For the substrate, Eq. (2.19) gives the Laplace transform of the relation between the surface traction and the surface displacement. Substituting Eqs. (4.16) and (4.17) into the continuity conditions (2.20) and (2.21) and then into Eq. (2.19), we obtain that

$$s\bar{\delta}(s) = \frac{E_f}{\bar{\mu}(s)}\left(\alpha - \frac{3\gamma_{22}k_0^3 h_f A_0^2}{8(1-\nu_f^2)}\right)\bar{\delta}(s) - \frac{\gamma_{22}p_0}{2k_0 s\bar{\mu}(s)} - A_0, \tag{4.19}$$

where α is given by Eq. (4.7). Again, we assume that the Poisson's ratio of the substrate is independent of time, and use the first two terms in Eq. (4.8) for the relaxation modulus. Substituting the first two terms of Eq. (4.9) into Eq. (4.19), we obtain that, after rearranging,

$$s\bar{\delta}(s) = \frac{\alpha' E_f - \mu_\infty}{\mu_0 - \alpha' E_f} p_1 \bar{\delta}(s) + \frac{\mu_0 - \mu_\infty}{\mu_0 - \alpha' E_f}\frac{p_1}{s} A_0, \tag{4.20}$$

where

$$\alpha' = \alpha - \frac{3\gamma_{22}k_0^3 h_f A_0^2}{8(1-\nu_f^2)}. \tag{4.21}$$

At the limit of a thick substrate ($H/h_f \to \infty$), using Eqs. (4.1), (4.7), and (4.15), we obtain

$$\alpha' = \frac{\mu_0}{E_f}\left(4 - 3\frac{\sigma_0}{\sigma_{c0}}\right). \tag{4.22}$$

Inverse transform of Eq. (4.20) leads to

$$\frac{d\delta}{dt} = \frac{\alpha' E_f - \mu_\infty}{\mu_0 - \alpha' E_f} p_1 \delta(t) + \frac{\mu_0 - \mu_\infty}{\mu_0 - \alpha' E_f} p_1 A_0. \tag{4.23}$$

Solving Eq. (4.23), we obtain the wrinkle amplitude as a function of time

$$A(t) = A_0 + A_0 \frac{\mu_0 - \mu_\infty}{\alpha' E_f - \mu_\infty}\left[\exp\left(\frac{\alpha' E_f - \mu_\infty}{\mu_0 - \alpha' E_f} p_1 t\right) - 1\right]. \tag{4.24}$$

Solution (4.24) only applies for large compressive stress (i.e., $|\sigma_0| > |\sigma_{c0}|$), because the initial equilibrium amplitude A_0 would be imaginary otherwise. For an elastic substrate ($\mu_0 = \mu_\infty$), the wrinkle amplitude becomes a constant as expected. For a viscoelastic substrate, depending on the stress level, there are three characteristic growth behaviors. When $\alpha' > \mu_\infty/E_f$, the growth is accelerating. When $\alpha' < \mu_\infty/E_f$, the growth is decelerating. In between, when $\alpha' = \mu_\infty/E_f$, the wrinkle grows linearly with time. The parameter α' decreases as the stress increases, and $\alpha' < \mu_0/E_f$ when $|\sigma_0| > |\sigma_{c0}|$. Fig. 14 shows the three growth behaviors for an elastic film on a thick

viscoelastic substrate ($H/h_f \to \infty$), where the stress for linear growth is given by

$$\sigma_0^* = \frac{4}{3}\sigma_{c0}\left(1 - \frac{\mu_\infty}{4\mu_0}\right). \tag{4.25}$$

The above linear perturbation analysis is only valid for a short time at the initial stage of kinetic wrinkling. The wrinkle amplitude eventually saturates at the equilibrium state corresponding to the rubbery limit. Subsequently, the wavelength and the amplitude of wrinkle evolve simultaneously, toward the energetically selected mode ($L_0 \to L_\infty$) for an elastic substrate with the rubbery modulus. The subsequent evolution is kinetically constrained and may take a long time. A nonlinear analysis is needed to further understand the process of mode transition.

5. Conclusion

This paper studies the wrinkling process of compressed elastic films on viscoelastic substrates, where both energetics and kinetics play important roles. Depending on the stress level in the film and the viscoelastic property of the substrate, the film can be stable or unstable, and, for the unstable cases, can grow wrinkles kinetically or first dynamically then kinetically. At different stress levels, the wrinkling kinetics is different. Fig. 15 summarizes the wrinkling kinetics in a schematic map spanning the glassy modulus of the substrate and the compressive stress in the film, assuming a constant ratio between the rubbery modulus and the glassy modulus. The three

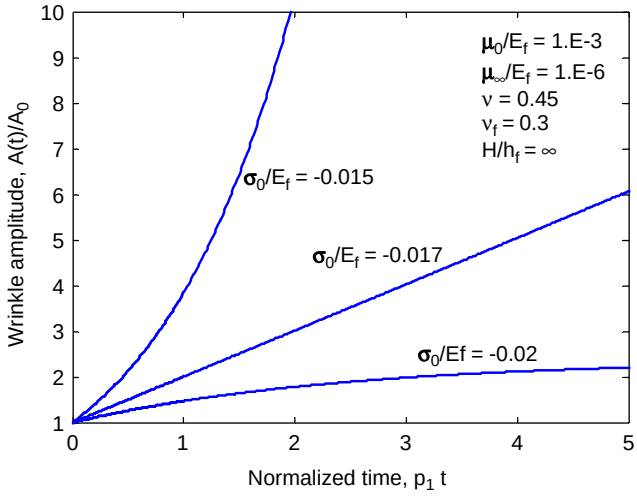

Fig. 14. Three characteristic wrinkling behaviors of an elastic film, subjected to large stresses, on a thick viscoelastic substrate ($H/h_f \to \infty$): accelerating growth ($\sigma_0/E_f = -0.015$), linear growth ($\sigma_0/E_f = -0.017$), and decelerating growth ($\sigma_0/E_f = -0.02$).

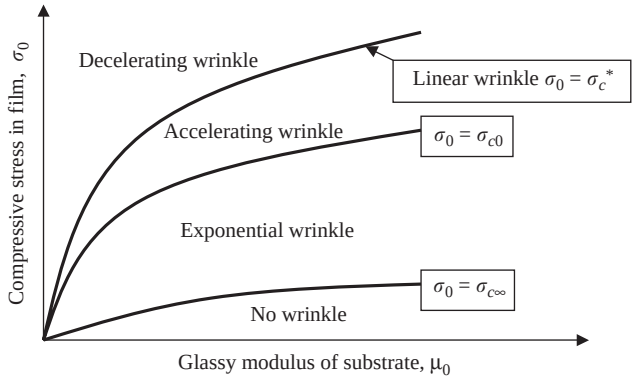

Fig. 15. A schematic map of the wrinkling kinetics for a compressed elastic film on a viscoelastic substrate.

boundary lines in the map are robustly defined by the elastic properties of the substrate at the glassy and rubbery limits, e.g., Eqs. (4.1), (4.2), and (4.25) for thick substrates. Of particular interest is the selection of a wavelength at the initial stage and the transition to another wavelength after a long time. The results from the present study may be used to characterize viscoelastic properties of thin polymer films and to control the length scale of the ordered patterns generated by wrinkling of an elastic film on a polymeric substrate.

The present study has focused on the wrinkling kinetics at the initial stage. Modeling long time evolution of wrinkles requires a nonlinear analysis. Furthermore, a blanket film often wrinkles in all directions, for which the plane strain condition does not hold. Results from nonlinear analyses on buckling blisters of debonded films (Ortiz and Gioia, 1994, 1997; Belgacem et al., 2000, 2002) may help subsequent studies of wrinkling on viscoelastic substrates in the nonlinear regime. Shortly after this paper was submitted, a numerical method was developed to simulate the evolution of two-dimensional wrinkle patterns by assuming a simplified viscoelastic behavior for the substrate (Huang et al., 2004a, b). Comparisons between the linear and nonlinear analyses as well as between modeling and experiments are in progress to further understand the evolution of wrinkling patterns.

Acknowledgements

The author is grateful for the support by the NSF through grant CMS-0412851 and by College of Engineering of The University of Texas at Austin. Discussions with Professor K.M. Liechti (UT-Austin) and Professor Z. Suo (Harvard University) were helpful.

Appendix A. Solution to an elastic layer under periodic surface tractions

Consider an elastic layer of thickness H subjected to plane strain deformation. The elastic boundary value problem can be solved by using the stress and displacement potentials, following the similar procedures in Huang and Suo (2002b) for a viscous layer. The general solution to the stresses and displacements are

$$\sigma_{22} = -[C_1\cosh(ky) + C_2\sinh(ky) + C_3 ky\cosh(ky) + C_4 ky\sinh(ky)]\cos(kx), \tag{A.1}$$

$$\sigma_{21} = \begin{bmatrix} C_1\sinh(ky) + C_2\cosh(ky) \\ +C_3(\cosh(ky) + ky\sinh(ky)) + C_4(\sinh(ky) + ky\cosh(ky)) \end{bmatrix} \times \sin(kx), \tag{A.2}$$

$$u_1 = \frac{1}{2\mu k}\begin{bmatrix} C_1\cosh(ky) + C_2\sinh(ky) + C_3\left(\frac{1+\kappa}{2}\sinh(ky) + ky\cosh(ky)\right) \\ +C_4\left(\frac{1+\kappa}{2}\cosh(ky) + ky\sinh(ky)\right) \end{bmatrix} \times \sin(kx), \tag{A.3}$$

$$u_2 = -\frac{1}{2\mu k}\begin{bmatrix} C_1\sinh(ky) + C_2\cosh(ky) + C_3\left(\frac{1-\kappa}{2}\cosh(ky) + ky\sinh(ky)\right) \\ +C_4\left(\frac{1-\kappa}{2}\sinh(ky) + ky\cosh(ky)\right) \end{bmatrix} \times \cos(kx), \tag{A.4}$$

where $\kappa = 3 - 4\nu$, μ is the shear modulus, and ν the Poisson's ratio.

Assume the bottom surface is fixed and the top surface is subjected to a periodic traction, namely

$$u_2 = u_1 = 0 \text{ at } y = -H. \tag{A.5}$$

$$\sigma_{22} = A_2\cos kx \quad \text{and} \quad \sigma_{21} = A_1\sin kx \text{ at } y = 0. \tag{A.6}$$

Applying the boundary conditions, we obtain

$$C_1 = -A_2, \tag{A.7}$$

$$C_2 = -\frac{(kH)^2 - (1-\kappa^2)/4}{\kappa\cosh^2(kH) + (kH)^2 + ((1-\kappa)/2)^2}A_1 - \frac{(\kappa/2)\sinh(2kH) - kH}{\kappa\cosh^2(kH) + (kH)^2 + ((1-\kappa)/2)^2}A_2, \tag{A.8}$$

$$C_3 = \frac{\kappa\cosh^2(kH) + (1-\kappa)/2}{\kappa\cosh^2(kH) + (kH)^2 + ((1-\kappa)/2)^2} A_1 + \frac{(\kappa/2)\sinh(2kH) - kH}{\kappa\cosh^2(kH) + (kH)^2 + ((1-\kappa)/2)^2} A_2, \tag{A.9}$$

$$C_4 = \frac{(\kappa/2)\sinh(2kH) + kH}{\kappa\cosh^2(kH) + (kH)^2 + ((1-\kappa)/2)^2} A_1 + \frac{\kappa\cosh^2(kH) + (1-\kappa)/2}{\kappa\cosh^2(kH) + (kH)^2 + ((1-\kappa)/2)^2} A_2. \tag{A.10}$$

Substituting Eqs. (A.7)–(A.10) into Eqs. (A.3) and (A.4), we obtain the displacements at the top surface (i.e., $y = 0$):

$$u_1(x,0) = \frac{1}{2\mu k}[\gamma_{11}A_1 + \gamma_{12}A_2]\sin(kx), \tag{A.11}$$

$$u_2(x,0) = \frac{1}{2\mu k}[\gamma_{21}A_1 + \gamma_{22}A_2]\cos(kx), \tag{A.12}$$

where the dimensionless coefficients are given by

$$\gamma_{11} = \frac{1+\kappa}{4}\frac{\kappa\sinh(2kH) + 2kH}{\kappa\cosh^2(kH) + (kH)^2 + ((1-\kappa)/2)^2}, \tag{A.13}$$

$$\gamma_{22} = \frac{1+\kappa}{4}\frac{\kappa\sinh(2kH) - 2kH}{\kappa\cosh^2(kH) + (kH)^2 + ((1-\kappa)/2)^2}, \tag{A.14}$$

$$\gamma_{12} = \gamma_{21} = -\frac{(\kappa(1-\kappa)/2)\sinh^2(kH) + (kH)^2}{\kappa\cosh^2(kH) + (kH)^2 + ((1-\kappa)/2)^2}. \tag{A.15}$$

For an infinitely thick elastic layer ($kH \to \infty$), Eqs. (A.11) and (A.12) become

$$u_1(x,0) = \frac{1}{2\mu k}[2(1-\nu)A_1 + (1-2\nu)A_2]\sin(kx), \tag{A.16}$$

$$u_2(x,0) = \frac{1}{2\mu k}[(1-2\nu)A_1 + 2(1-\nu)A_2]\cos(kx). \tag{A.17}$$

Furthermore, if the elastic material is incompressible, i.e., $\nu = 0.5$, the surface displacements reduce to

$$u_1(x,0) = \frac{1}{2\mu k}A_1\sin(kx), \tag{A.18}$$

$$u_2(x,0) = \frac{1}{2\mu k}A_2\cos(kx). \tag{A.19}$$

In this special case ($kH \to \infty$ and $\nu = 0.5$), the shear and normal surface displacements are decoupled, namely, a normal traction causes only normal

displacement at the surface and a shear traction causes only shear displacement at the surface. In general, however, the two displacements are coupled as in Eqs. (A.11) and (A.12).

Appendix B. Energetics for wrinkling of elastic films on elastic substrates

Consider an elastic film on an elastic substrate. Assume a sinusoidal wrinkle (Eq. (2.4)), and neglect in-plane displacement. The elastic strain energy in the film consists of two parts, corresponding to bending and in-plane compression, respectively. The energy densities (energy per unit area of a flat film) are given by

$$U_{\mathrm{B}} = \frac{E_{\mathrm{f}} h_{\mathrm{f}}^3}{24(1-\nu_{\mathrm{f}}^2)} \left(\frac{\partial^2 w}{\partial x^2}\right)^2, \tag{B.1}$$

$$U_{\mathrm{C}} = \frac{(1-\nu)\sigma_0^2 h_{\mathrm{f}}}{E_{\mathrm{f}}} + \frac{1}{2}\sigma_0 h_{\mathrm{f}} \left(\frac{\partial w}{\partial x}\right)^2 + \frac{E_{\mathrm{f}} h_{\mathrm{f}}}{8(1-\nu_{\mathrm{f}}^2)} \left(\frac{\partial w}{\partial x}\right)^4. \tag{B.2}$$

The strain energy in the substrate equals the work done by the surface traction, namely

$$U_{\mathrm{s}} = \frac{1}{2} S_2(x) u_2(x,0). \tag{B.3}$$

By the continuity condition (2.20) and relation (3.1), we have

$$U_{\mathrm{s}} = \frac{1}{\gamma_{22}} \mu k w^2, \tag{B.4}$$

where γ_{22} is given by (A.14).

Substituting Eq. (2.4) into Eqs. (B.1), (B.2), and (B.4) and integrating over one period of the wrinkle and then dividing by the wavelength, we obtain the average strain energy per unit area:

$$\bar{U}_{\mathrm{B}} = \frac{E_{\mathrm{f}} h_{\mathrm{f}}^3}{48(1-\nu_{\mathrm{f}}^2)} k^4 A^2, \tag{B.5}$$

$$\bar{U}_{\mathrm{C}} = \frac{(1-\nu)\sigma_0^2 h_{\mathrm{f}}}{E_{\mathrm{f}}} + \frac{1}{4}\sigma_0 h_{\mathrm{f}} k^2 A^2 + \frac{3E_{\mathrm{f}} h_{\mathrm{f}}}{64(1-\nu_{\mathrm{f}}^2)} k^4 A^4, \tag{B.6}$$

$$\bar{U}_{\mathrm{s}} = \frac{1}{2\gamma_{22}} \mu k A^2. \tag{B.7}$$

For a given wave number k, minimizing the total energy, we obtain

$$A_e = \frac{2\sqrt{6(1-\nu_f^2)}}{3k}\left[-\frac{\sigma_0}{E_f} - \frac{(kh_f)^2}{12(1-\nu_f^2)} - \frac{2}{\gamma_{22}}\frac{\mu}{E_f}\frac{1}{kh_f}\right]^{1/2}, \tag{B.8}$$

which is slightly smaller than the equilibrium amplitude in Eq. (3.2) as noted before.

Substituting Eq. (B.8) into Eqs. (B.5)–(B.7) and further minimizing the total strain energy with respect to k, we obtain the wave number that minimizes the total strain energy, which takes the form

$$k_m = \frac{1}{h_f}\Phi\left(\frac{\mu}{E_f}, \frac{H}{h_f}, \nu, \nu_f\right), \tag{B.9}$$

where the dimensionless number Φ is independent of the film stress. In the limiting case for a thick substrate ($H/h_f \to \infty$), (B.9) reduces to

$$k_m = \frac{1}{h_f}\left[\frac{6(1-\nu_f^2)}{1-\nu}\frac{\mu}{E_f}\right]^{1/3}. \tag{B.10}$$

In the other limiting case for a thin substrate ($H/h_f \to 0$), Eq. (B.9) reduces to

$$k_m = \frac{1}{h_f}\left[\frac{24(1-\nu_f^2)(1-\nu)}{1-2\nu}\frac{\mu}{E_f}\frac{h_f}{H}\right]^{1/4}. \tag{B.11}$$

The corresponding wrinkle amplitude of the selected wave number can be obtained by substituting Eq. (B.9) into Eq. (B.8).

References

Allen, H.G., 1969. Analysis and Design of Structural Sandwich Panels. Pergamon Press, New York.

Balint, D.S., Hutchinson, J.W., 2003. Undulation instability of a compressed elastic film on a nonlinear creeping substrate. Acta Mater. 51, 3965–3983.

Belgacem, H.B., Conti, S., DeSimone, A., Muller, S., 2000. Rigorous bounds for the Foppl-von Karman theory of isotropically compressed plates. J. Nonlinear Sci. 10, 661–683.

Belgacem, H.B., Conti, S., DeSimone, A., Muller, S., 2002. Energy scaling of compressed elastic films—three-dimensional elasticity and reduced theories. Arch. Rat. Mech. Anal. 164, 1–37.

Bowden, N., Brittain, S., Evans, A.G., Hutchinson, J.W., Whitesides, G.M., 1998. Spontaneous formation of ordered structures in thin films of metals supported on an elastomeric polymer. Nature 393, 146–149.

Bowden, N., Huck, W.T.S., Paul, K.E., Whitesides, G.M., 1999. The controlled formation of ordered, sinusoidal structures by plasma oxidation of an elastomeric polymer. Appl. Phys. Lett. 75 (17), 2557–2559.

Cerda, E., Mahadevan, L., 2003. Geometry and physics of wrinkling. Phys. Rev. Lett. 90 (7), 074302.

Chen, X., Hutchinson, J.W., 2004. Herringbone buckling patterns of compressed thin films on compliant substrates. J. Appl. Mech., in press

Christensen, R.M., 1982. Theory of Viscoelasticity: An Introduction. Academic Press, New York.

Chua, D.B.H., Ng, H.T., Li, S.F.Y., 2000. Spontaneous formation of complex and ordered structures on oxygen-plasma-treated elastomeric polydimethylsiloxane. Appl. Phys. Lett. 76 (6), 721–723.

Gioia, G., DeSimone, A., Ortiz, M., Cuitino, A.M., 2002. Folding energetics in thin-film diaphragms. Proc. R. Soc. London A 458, 1223–1229.

Groenewold, J., 2001. Wrinkling of plates coupled with soft elastic media. Physica A 298, 32–45.
He, M.Y., Evans, A.G., Hutchinson, J.W., 2000. The ratcheting of compressed thermally grown thin films on ductile substrates. Acta Mater. 48, 2593–2601.
Hobart, K.D., Kub, F.J., Fatemi, M., Twigg, M.E., Thompson, P.E., Kuan, T.S., Inoki, C.K., 2000. Compliant substrates: a comparative study of the relaxation mechanisms of strained films bonded to high and low viscosity oxides. J. Electron. Mater. 29, 897–900.
Huang, R., Suo, Z., 2002a. Wrinkling of a compressed elastic film on a viscous layer. J. Appl. Phys. 91, 1135–1142.
Huang, R., Suo, Z., 2002b. Instability of a compressed elastic film on a viscous layer. Int. J. Solids Struct. 39, 1791–1802.
Huang, Z.Y., Hong, W., Suo, Z., 2004a. Evolution of wrinkles in hard films on soft substrates. Submitted.
Huang, Z.Y., Hong, W., Suo, Z., 2004b. Nonlinear analysis of wrinkles in films on soft elastic substrates. Submitted.
Huck, W.T.S., Bowden, N., Onck, P., Pardoen, T., Hutchinson, J.W., Whitesides, G.M., 2000. Ordering of spontaneously formed buckles on planar surfaces. Langmuir 16, 3497–3501.
Hutchinson, J.W., Suo, Z., 1992. Mixed-mode cracking in layered materials. Adv. Appl. Mech. 29, 63–191.
Iacopi, F., Brongersma, S.H., Maex, K., 2003. Compressive stress relaxation through buckling of a low-k polymer-thin cap layer system. Appl. Phys. Lett. 82 (9), 1380–1382.
Im, S.H., Huang, R., 2004. Ratcheting-induced wrinkling of an elastic film on a metal layer under cyclic temperatures. Acta Mater. 52, 3707–3719.
Jones, J., Lacour, S.P., Wagner, S., Suo, Z., 2003. A method for making elastic metal interconnects. Mater. Res. Soc. Symp. Proc. 769, H6.12.
Karlsson, A.M., Evans, A.G., 2001. A numerical model for the cyclic instability of thermally grown oxides in thermal barrier systems. Acta Mater. 49, 1793–1804.
Lacour, S.P., Wagner, S., Huang, Z.Y., Suo, Z., 2003. Stretchable gold conductors on elastomeric substrates. Appl. Phys. Lett. 82 (15), 2404–2406.
Landau, L.D., Lifshitz, E.M., 1959. Theory of Elasticity. Pergamon Press, London.
Lu, Y.F., Choi, W.K., Aoyagi, Y., Kinomura, A., Fujii, K., 1996. Controllable laser-induced periodic structures at silicon-dioxide/silicon interface by excimer laser irradiation. J. Appl. Phys. 80 (12), 7052–7056.
Muller-Wiegand, M., Georgiev, G., Oesterschulze, E., Fuhrmann, T., Salbeck, J., 2002. Spinodal patterning in organic–inorganic hybrid layer systems. Appl. Phys. Lett. 81 (26), 4940–4942.
Mumm, D.R., Evans, A.G., Spitsberg, I.T., 2001. Characterization of a cyclic displacement instability for a thermally grown oxide in a thermal barrier system. Acta Mater. 49, 2329–2340.
Ortiz, M., Gioia, G., 1994. The morphology and folding patterns of buckling-driven thin-film blisters. J. Mech. Phys. Solids 42, 531–559.
Ortiz, M., Gioia, G., 1997. Delamination of compressed thin films. Adv. Appl. Mech. 33, 119–192.
Serrano, J.R., Cahill, D.G., 2002. Micron-scale buckling of SiO_2 on Si. J. Appl. Phys. 92 (12), 7606–7610.
Sridhar, N., Srolovitz, D.J., Suo, Z., 2001. Kinetics of buckling of a compressed lm on a viscous substrate. Appl. Phys. Lett. 78, 2482–2484.
Sridhar, N., Srolovitz, D.J., Cox, B.N., 2002. Buckling and post-buckling kinetics of compressed thin films on viscous substrates. Acta Mater. 50, 2547–2557.
Suo, Z., 1995. Wrinkling of the oxide scale on an aluminum-containing alloy at high temperatures. J. Mech. Phys. Solids 43, 829–846.
Timoshenko, S., Woinowsky-Krieger, S., 1987. Theory of Plates and Shells. second ed, McGraw-Hill, New York.
Tolpygo, V.K., Clarke, D.R., 1998. Wrinkling of α-aluminum films grown by thermal oxidation I: Quantitative studies on single crystals of FeCrAl alloy. Acta Mater. 46 (14), 5153–5166.
Watanabe, M., Shirai, H., Hirai, T., 2002. Wrinkled polypyrrole electrode for electroactive polymer actuators. J. Appl. Phys. 92 (8), 4631–4637.

Yin, H., Huang, R., Hobart, K.D., Suo, Z., Kuan, T.S., Inoki, C.K., Shieh, S.R., Duffy, T.S., Kub, F.J., Sturm, J.C., 2002. Strain relaxation of SiGe islands on compliant oxide. J. Appl. Phys. 91, 9716–9722.

Yoo, P.J., Lee, H.H., 2003. Evolution of a stress-driven pattern in thin bilayer films: spinodal wrinkling. Phys. Rev. Lett. 91 (15), 154502.

Yoo, P.J., Suh, K.Y., Park, S.Y., Lee, H.H., 2002. Physical self-assembly of microstructures by anisotropic buckling. Adv. Mater. 14 (19), 1383–1387.